Targeted Indocyanine-Green-Loaded Calcium Phosphosilicate Nanoparticles for *In Vivo* Photodynamic Therapy of Leukemia

Brian M. Barth,[†,*] Erhan İ. Altınoğlu,[‡] Sriram S. Shanmugavelandy,[†] James M. Kaiser,[†] Daniza Crespo-Gonzalez,[§] Nicole A. DiVittore,[†,⊥] Christopher McGovern,[∥] Trevor M. Goff,[‡] Nicole R. Keasey,[⊥,∥] James H. Adair,[‡] Thomas P. Loughran, Jr.,[⊥,∥] David F. Claxton,[⊥,∥] and Mark Kester[†,⊥,*]

[†]Department of Pharmacology, Pennsylvania State University College of Medicine, Hershey, Pennsylvania 17033, United States, [‡]Department of Materials Science and Engineering, Pennsylvania State University, University Park, Pennsylvania 16802, United States, [§]Department of Chemistry, University of Puerto Rico Mayaguez Campus, Mayaguez, Puerto Rico 00681, and [⊥]Penn State Hershey Cancer Institute and [∥]Department of Medicine, Pennsylvania State University College of Medicine, Hershey, Pennsylvania 17033, United States

ABSTRACT Leukemia is one of the most common and aggressive adult cancers, as well as the most prevalent childhood cancer. Leukemia is a cancer of the hematological system and can be divided into a diversity of unique malignancies based on the onset of the disease as well as the specific cell lineages involved. Cancer stem cells, including recently identified leukemia stem cells (LSCs), are hypothesized to be responsible for cancer development, relapse, and resistance to treatment, and new therapeutics targeting these cellular populations are urgently needed. Nontoxic and nonaggregating calcium phosphosilicate nanoparticles (CPSNPs) encapsulating the near-infrared fluoroprobe indocyanine green (ICG) were recently developed for diagnostic imaging and drug delivery as well as for photodynamic therapy (PDT) of solid tumors. Prior studies revealed that specific targeting of CPSNPs allowed for enhanced accumulation within breast cancer tumors, *via* CD71 targeting, or pancreatic cancer tumors, *via* gastrin receptor targeting. In the present study, ICG-loaded CPSNPs were evaluated as photosensitizers for PDT of leukemia. Using a novel bioconjugation approach to specifically target CD117 or CD96, surface features enhanced on leukemia stem cells, *in vitro* ICG-CPSNP PDT of a murine leukemia cell line and human leukemia samples were dramatically improved. Furthermore, the *in vivo* efficacy of PDT was dramatically enhanced in a murine leukemia model by utilizing CD117-targeted ICG-CPSNPs, resulting in 29% disease-free survival. Altogether, this study demonstrates that leukemia-targeted ICG-loaded CPSNPs offer the promise to effectively treat relapsing and multidrug-resistant leukemia and to improve the life of leukemia patients.

KEYWORDS: calcium phosphosilicate nanoparticles · photodynamic therapy · leukemia · leukemia stem cells · bioconjugation

Leukemia is a cancer of the blood, or bone marrow, usually characterized by an abnormal proliferation of white blood cells.[1,2] Myeloid leukemia refers to that developing from myeloblasts, while lymphocytic leukemias develop from lymphoblasts. Leukemia is the most common form of pediatric cancer, accounting for about one-third of all pediatric cases according to the American Cancer Society. Acute leukemia onsets rapidly and is the most common pediatric leukemia. Acute lymphocytic leukemia accounts for about 60% and acute myeloid leukemia for about 38% of childhood leukemia. Prognosis of childhood leukemia has improved recently, but survival rates remain around only 60%. Unfortunately, this moderate survival rate is only achieved by intensive therapy, which in itself results in high rates of mortality. Multidrug resistance, and relapse, is a particular problem in both adult and childhood leukemia and is a nearly certain predictor of a fatal outcome.[1,2] Recent studies have indicated the presence of small populations of cells within solid and nonsolid tumors with stem cell-like characteristics.[3−6] These cancer stem cells not only exhibit markers resembling embryonic and adult stem cells but also are fully capable of initiating tumor growth *in vivo*. Normal hematopoietic stem cells contain unique surface markers, and these same markers, $CD34^{+}CD38^{-}$, are also present in leukemia stem cells (LSCs). In particular, LSCs from acute myeloid leukemia (AML) patients were shown to be enriched into a $CD34^{+}CD38^{-}CD96^{+}$ cellular population.[7] Likewise, recent studies have indicated that LSCs reside within a $lineage^{-}Sca\text{-}1^{+}CD117^{+}$ cellular population in patients and models of chronic myeloid leukemia (CML).[8,9] Interestingly, these distinct populations of cells show hallmarks associated with multidrug resistance, and it is believed that these cells are responsible for leukemia relapse.[6]

Photodynamic therapy (PDT) has been described as an alternative to chemotherapy

* Address correspondence to bmb14@psu.edu, mkester@psu.edu.

Received for review February 12, 2011 and accepted June 15, 2011.

Published online June 15, 2011
10.1021/nn2005766

or radiation therapy for the treatment of malignant tumors.[10−12] PDT consists of three components: a photosensitizer, light, and oxygen. When exposed to light of a specific wavelength, a photosensitizer is excited, and a subsequent energy transfer to molecular oxygen produces highly reactive singlet oxygen which can lead to cell death.[12−14] The disadvantages of PDT are mostly associated with short lifetimes of photosensitizers, an inability to penetrate a sufficient number of photons through tissue, photosensitizer toxicity, and an inability to preferentially target cancerous tissues with photosensitizers.[14−17] PDT has benefited from recent developments in nanotechnology. Various polymeric and nonpolymeric nanoparticles have been reported to encapsulate or be conjugated to photosensitizers.[18−25] These nanoparticles have been evaluated both *in vitro* and *in vivo* and have been shown to improve the efficacy of PDT while decreasing toxicity. However, successful *in vivo* PDT is still limited to solid tumors residing in locations accessible to a light source. For example, successful PDT of glioblastoma in an orthotopic rat model using polymeric nanoparticles made of polyacrylamide was recently accomplished in part because the laser source was introduced through a hole created in the skull during surgery.[18] This study was noteworthy in comparison to many *in vivo* studies which typically rely on subcutaneous solid tumor engraftments. In contrast, there are several reports of successful PDT of leukemia *in vitro*, but these studies have not been extended to true *in vivo* models of leukemia where the disease is in systemic circulation.[26−29] The best attempt was a recent study which reported the utility of PDT to purge leukemic cells from autologous hematopoietic stem cells *ex vivo* prior to transplant.[30] As a nonsolid cancer of the blood and bone marrow, leukemia presents a challenge to photosensitizer or nanoparticle uptake that does not exist for solid tumors where their vasculature contributes to uptake through the enhanced permeation and retention effect.[31] Additionally, manifestation of leukemia throughout the body creates added challenges to the successful delivery of light needed for PDT.

The recent development of calcium phosphosilicate nanoparticles (CPSNPs) allowed for improved optical and quantum properties of encapsulated dyes, as well as protection during systemic delivery, until pH-dependent release during endocytosis.[32−35] CPSNPs offer a distinct advantage over similar nanoparticles because dyes, drugs, or other molecules of interest are efficiently encapsulated within the nanomatrix composed of calcium phosphosilicate. This is in contrast to surface decoration of the nanoparticle which can be the case for calcium phosphate-based systems.[36] Furthermore, calcium and phosphate are abundant in physiological systems and pose no inherent toxicity, whereas constituent components of some other nanoparticles, such as cadmium, selenium, or heavy metals, are significantly toxic and as such cannot be effectively used in biomedical applications. CPSNPs loaded with the near-infrared fluorescing dye indocyanine green (ICG) have recently been described. Initial studies showed that ICG-loaded CPSNPs functionalized with polyethylene glycol (PEG) effectively accumulated within, and imaged, breast and pancreatic cancer tumors in both subcutaneous and orthotopic *in vivo* models.[32,37] In comparison, free ICG was not able to effectively image tumors, which was directly reflective of enhanced fluorescence quantum efficiency (Φ_F) and photostability of ICG once encapsulated within CPSNPs. *In vivo* imaging was further improved by targeting CPSNPs specifically to CD71 on breast cancer tumors or to the gastrin receptor on pancreatic cancer tumors.[37] In a more recent study, the Φ_F values of free ICG and nanoencapsulated ICG were directly compared.[38] Standard Φ_F measurements describe the smallest fluorescing unit which only reveals the Φ_F of a single nanoparticle and not its constituent-encapsulated fluorescent molecules. This study overcame that hurdle and demonstrated the Φ_F in PBS for free ICG (0.027 ± 0.001), a typical CPSNP loaded with ICG (0.053 ± 0.003), and ICG molecules encapsulated within CPSNPs (0.066 ± 0.004).[38] This study also determined that 6 ± 2 ICG molecules were encapsulated per typical CPSNP (16 nm average diameter).[38] Currently, ICG is used in imaging applications as an FDA-approved contrast agent.[39] The *in vivo* use of ICG suffers dramatically from a short plasma half-life (2−4 min), photobleaching, and nonspecific quenching due to binding with serum proteins.[40] The encapsulation of ICG within CPSNPs overcomes these hurdles and potentially expands the use of ICG beyond imaging to therapeutic applications such as PDT.

In this study, ICG-loaded CPSNPs were studied as photosensitizers in models of leukemia. The efficacy of ICG-CPSNP PDT was considered to be relative to the amount of nanoparticle endocytosed by cancerous cells. In the case of leukemia, it was speculated that untargeted ICG-CPSNPs would show only limited utility for PDT, as nanoparticles would not accumulate passively *via* enhanced permeation and retention like they would in solid tumors.[32,37] However, it was hypothesized that specific and selective targeting of ICG-CPSNPs would permit effective PDT of leukemia. Furthermore, it was predicted that PDT utilizing LSC-targeted ICG-CPSNPs would be particularly efficacious owing to the elimination of the specific leukemic cellular population responsible for the maintenance and progression of the disease.

RESULTS AND DISCUSSION

Novel Bioconjugation of CPSNPs. In prior studies, CPSNPs were specifically engineered to target CD71 or the gastrin receptor using avidin−biotin noncovalent coupling as well as covalent coupling using maleimide-terminated PEG.[37] The disadvantage of the

maleimide coupling approach is due to the reliance on the availability of thiol groups on the molecule to be conjugated. If thiols are unavailable, they must be introduced under conditions that may jeopardize the integrity of biomolecules. To avoid this potential problem, a multistep conjugation approach was employed to generate PEGylated CPSNPs containing sulfo-NHS (*N*-hydroxysuccinimide) ester groups, which were then reacted, at neutral pH, with antibodies selective for surface features on leukemic cells (Figure 1). In brief, citrate-functionalized CPSNPs were activated by 1-ethyl-3-(3-dimethylaminopropyl)-carbodiimide (EDAC) and then reacted with sulfo-NHS to form a high-yield, semistable intermediate. The sulfo-NHS ester-containing CPSNPs were then reacted with heterobifunctional PEG containing both amine and carboxyl functional groups. This synthetic process was repeated with the carboxyl-PEG functional terminals of the PEGylated CPSNPs to generate sulfo-NHS ester-containing PEGylated CPSNPs, which readily reacted with antibodies to form specifically targeted, PEGylated CPSNPs.

Previous studies have shown that effective PEGylation of citrate-CPSNPs neutralized the net charge of the nanoparticles.[32−34,37] As charged nanoparticles have been shown to be toxic in animal models,[41] it was important to show that the addition of specific targeting moieties did not introduce significant charge to the CPSNPs. Indeed, functionalization with specific antibodies yielded neutrally charged CPSNPs which were essentially identical in charge to their untargeted PEGylated counterparts (Figure 2A). Dynamic light scattering analysis showed an increase in CPSNP size as a consequence of the successful bioconjugation with antibodies targeting CD96 or CD117 (Figure 2B), which was confirmed by transmission electron microscopy (Figure 2B, inset).

Verification of the Presence of Leukemia Stem Cell Markers. In order to verify the potential utility of leukemia-targeted ICG-CPSNP PDT, LSCs were evaluated by flow

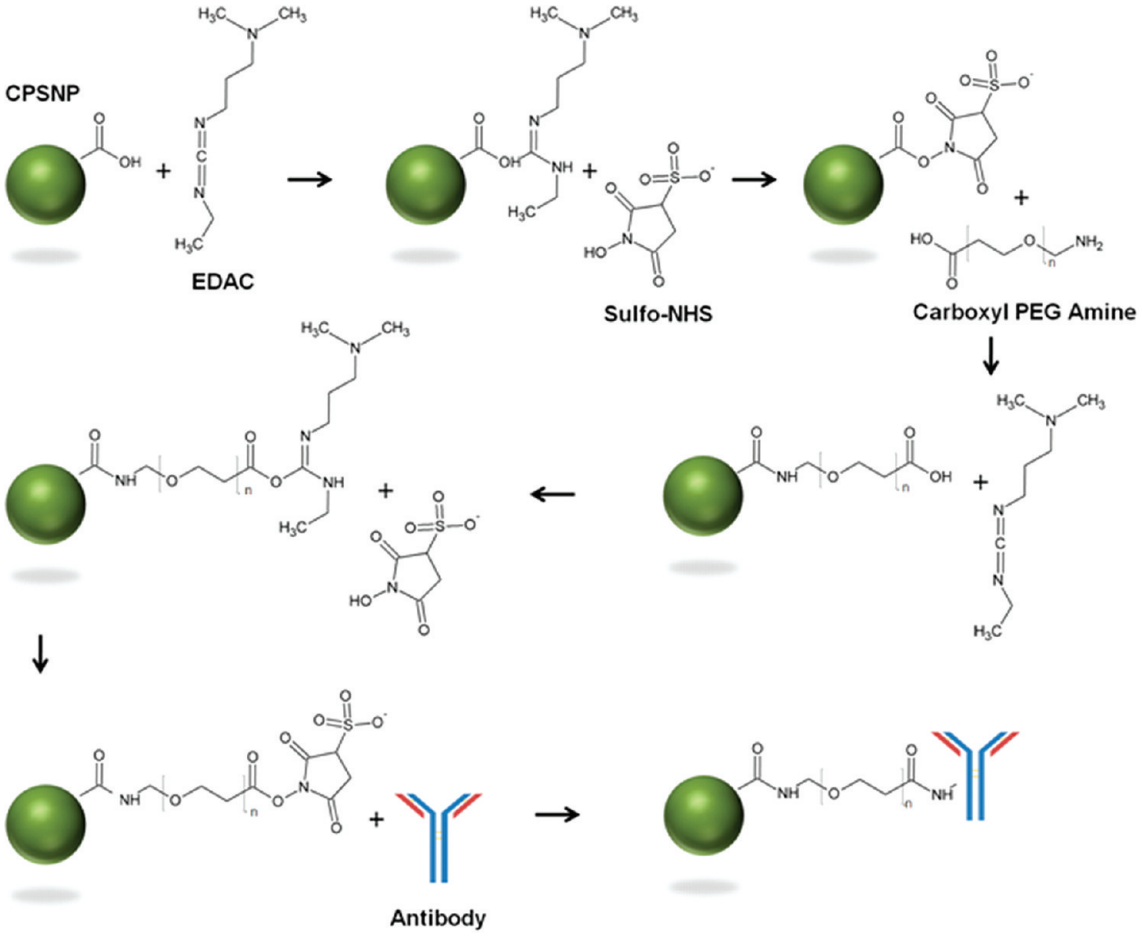

Figure 1. Schematic depicting multistep bioconjugation process, utilizing the generation of sulfo-NHS ester-containing PEGylated CPSNPs, by which targeting was achieved. Briefly, citrate-functionalized CPSNPs were activated by 1-ethyl-3-(3-dimethylaminopropyl)carbodiimide (EDAC) and then reacted with sulfo-NHS (*N*-hydroxysuccinimide) to form a high-yield, semistable intermediate. PEG, with both amine and carboxyl functional groups, was reacted with the sulfo-NHS ester-containing CPSNPs. The synthetic process was repeated with the carboxyl-PEG functional terminals of the PEGylated CPSNPs to generate sulfo-NHS ester-containing PEGylated CPSNPs, which readily reacted with antibodies, at neutral pH, to form specifically targeted, PEGylated CPSNPs.

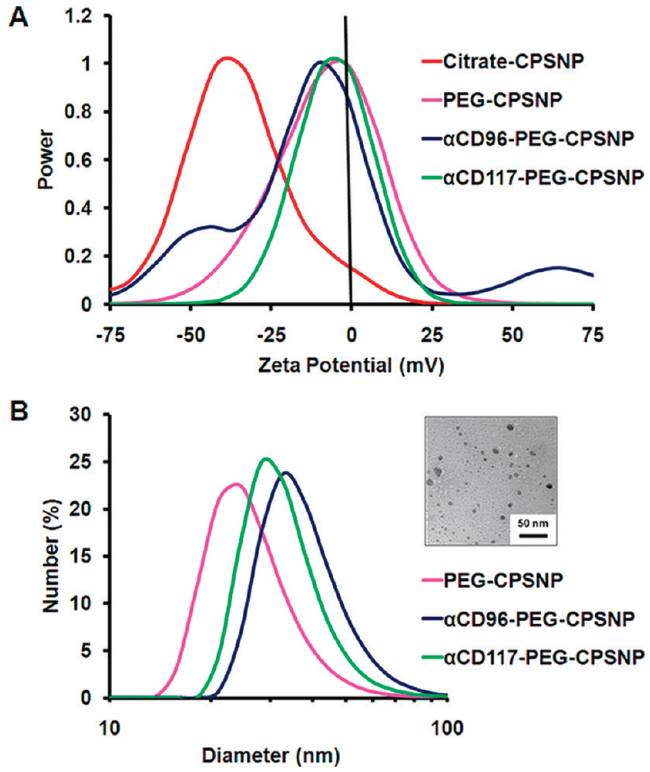

Figure 2. Physical characterization of LSC-targeted CPSNPs. (A) Zeta potential analysis showed negatively charged citrate-functionalized CPSNPs (starting point for synthesis). Untargeted PEGylated CPSNPs and PEGylated CPSNPs targeting CD96 or CD117 (with respective monoclonal antibody functionalization) were all neutral charged. (B) Dynamic light scattering (DLS) analysis showed an increase in CPSNP size as a consequence of the addition of monoclonal antibodies (targeting CD96 or CD117) to PEGylated CPSNPs. Transmission electron microscopy (TEM) was used to verify the size of CD117-targeted CPSNPs (inset).

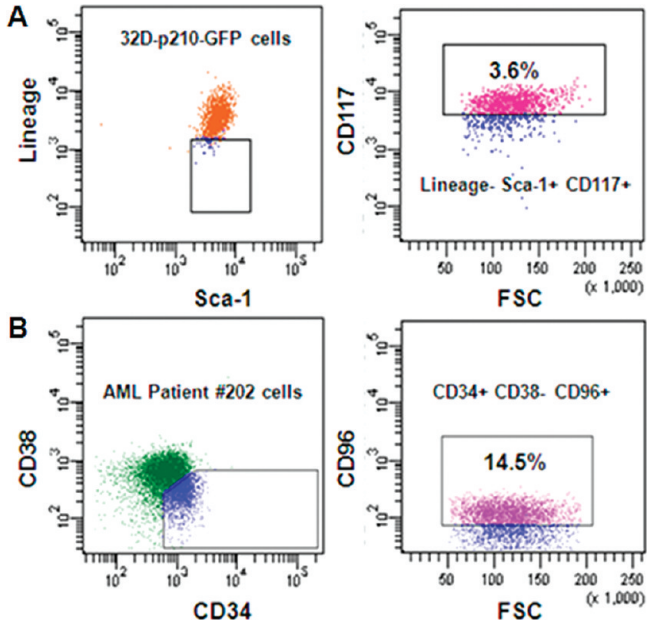

Figure 3. Presence of leukemia stem cell markers was verified by flow cytometry. (A) Lineage$^-$CD117$^+$Sca-1$^+$ chronic myeloid leukemia (CML) stem cell markers on 32D-p210-GFP cells (3.6% of cellular population). (B) CD34$^+$CD38$^-$CD96$^+$ acute myeloid leukemia (AML) stem cell markers on a patient's cells (14.5% of cellular population).

cytometry. Like other cancer stem cells, LSCs are thought to be major determinants to cancer development and, in particular, to multidrug resistance and to relapse following therapy.[3−6] Previous studies have characterized LSCs within a lineage$^-$Sca-1$^+$CD117$^+$ cellular population in CML,[8,9] while LSCs were

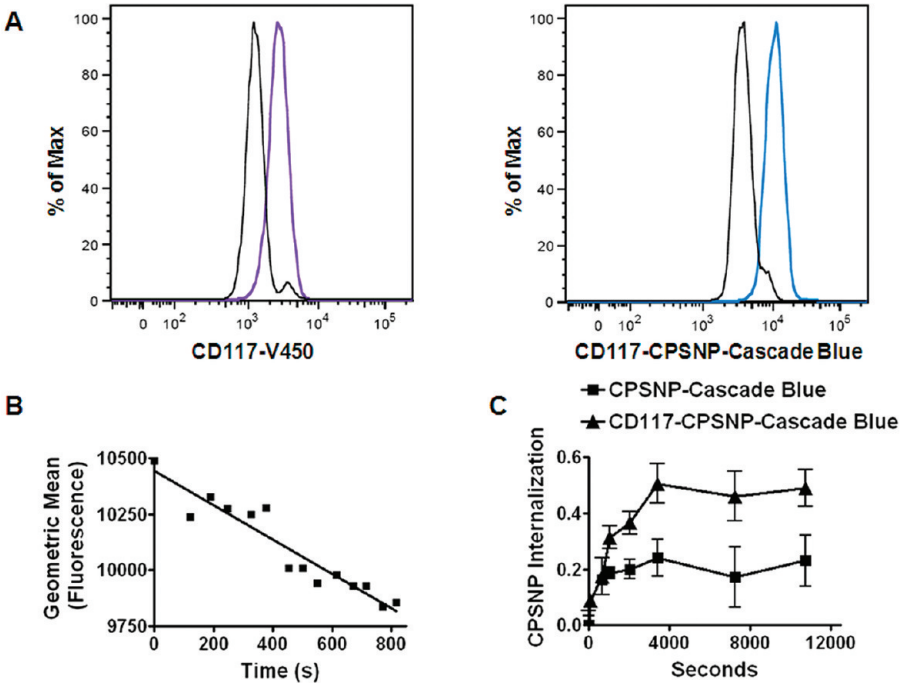

Figure 4. Cellular validation of targeted CPSNPs. (A) Flow cytometry was used to demonstrated that 32D-p210-GFP cells were effectively labeled with a V450-conjugated antibody specific for CD117 (left), which validated the effective targeting of Cascade-Blue-loaded CPSNPs conjugated with CD117-specific antibodies (right). (B) Decrease in the geometric mean of fluorescence, due to CPSNP internalization and pH-dependent dissolution within the endosomal–lysosomal pathway, was observed during flow cytometry using 32D-p210-GFP cells labeled with CD117-targeted CPSNPs loaded with Cascade Blue. (C) Fluorescent microplate assay was used to evaluate the internalization into 32D-p210-GFP cells of either untargeted, or CD117-targeted, Cascade-Blue-loaded CPSNPs. Internalization was quantified as a decrease in fluorescence in the presence of cells, minus the background decrease in fluorescence in the absence of cells.

characterized within a $CD34^+CD38^-CD96^+$ cellular population in AML.[7] LSCs have also been identified in both acute and chronic lymphoblastic leukemia. In this study, CML was modeled by using the murine 32D-p210-GFP cell line,[42,43] and human AML patient samples were also studied. Although the 32D-p210-GFP model is a CML model, it also behaves like AML with its rapid proliferation of immature leukemic blasts.[2,43] In the 32D-p210-GFP CML model, a small population of cells (3.6%) with $lineage^-Sca\text{-}1^+CD117^+$ surface characteristics was observed (Figure 3A). In comparison, cells from a human AML patient were observed to have a substantial percentage (14.5%) of purported $CD34^+CD38^-CD96^+$ LSCs (Figure 3B). Of importance, cancer stem cell populations have been observed to expand under conditions associated with treatment or in cases of more aggressive disease. The presence of these cellular populations verified the potential utility of LSC-targeted CPSNP development. Furthermore, if these populations were truly LSCs, it was hypothesized that selective targeting to CD117 or CD96 would result in a profound improvement in PDT efficacy utilizing ICG-CPSNPs due to the integral nature of LSCs to leukemia development, progression, and therapy resistance.

Validation of Leukemia Cell-Targeted CPSNPs. Flow cytometry and the loss of fluorescence during CPSNP internalization were used to validate the effective targeting of antibody-coupled CPSNPs. Cascade Blue-loaded CPSNPs were conjugated to anti-CD117 antibodies and directly compared to V450-conjugated anti-CD117 antibodies (BD Biosciences, San Jose, CA). Cascade Blue and V450 have similar spectra and were readily analyzed under the same filter conditions by flow cytometry. 32D-p210-GFP cells were effectively labeled and visualized using CD117-targeted Cascade Blue-loaded CPSNPs or V450-conjugated anti-CD117 antibodies (Figure 4A). In the case of fluorescent dyes, encapsulation within CPSNPs dramatically improves optical properties such as quantum yield and fluorescence lifetime. Dissolution of the CPSNPs once they have been internalized within the acidic environment of the lysosome may result in a loss of fluorescence depending on the stability of the dye used.[32,33,35,37] It is important to note that for certain dyes with low or moderate optical properties, despite enhancement by encapsulation in CPSNPs, internalization alone may decrease the observed fluorescence as the fluorescent dye moves away from the cellular surface. In the case of CD117-targeted Cascade Blue-loaded CPSNPs, a gradual loss in fluorescence was observed as they were internalized by 32D-p210-GFP cells. This loss of fluorescence due to internalization was revealed as a decrease in the geometric mean of fluorescence of the cellular population labeled by the targeted CPSNPs

(Figure 4B). To further study the kinetics of CPSNP internalization, a fluorescence microplate assay was performed with CD117-targeted or untargeted CPSNPs (Figure 4C). Internalization, revealed by a loss of fluorescence, was significantly greater for CD117-targeted CPSNPs than untargeted CPSNPs and reached a maximum after nearly 45 min.

The biological mechanisms responsible for internalization contribute to the efficacy of dye-loaded CPSNPs to behave as effective photosensitizers for PDT rather than immediately dissolving and losing optimal Φ_F. While untargeted CPSNPs likely enter cells *via* pinocytosis, CD117-targeted CPSNPs enter *via* receptor-mediated endocytosis. Receptor-mediated endocytosis can result in different intracellular trafficking as ligand-bound receptors have been shown to traffic from the plasma membrane to a variety of intracellular membranes and often are then recycled back to the plasma membrane.[44−47] It has been suggested that, during receptor-mediated endocytosis, early endosomes become "sorting centers", where different receptor complexes and their associated proteins may be trafficked to distinct locations for signal transduction purposes or recycled back to the plasma membrane.[46] CD117, a receptor tyrosine kinase also known as c-kit, is the receptor for stem cell factor (SCF) and is normally internalized by ligand binding.[48] CD117 internalization is dependent on tyrosine kinase activity, and this process has been shown to be important to the pro-growth signaling mechanisms elicited by SCF.[48−50] Studies have shown that ligand-bound and activated CD117 is internalized and ultimately trafficked to lysosomes where the receptor is degraded.[51,52] However, it is unclear how CD117 trafficking is altered when the ligand is not present or during cancer where nuclear localization has been reported.[52] Intriguingly, inhibitors of tyrosine kinases including those commonly used as first-line therapeutics for CML have been shown to prevent CD117 internalization and SCF-mediated pro-growth signaling.[48,53] Taken together, these mechanisms of internalization may maintain the physical integrity of dye-loaded CPSNPs to allow optimal Φ_F for PDT.

Generation of Singlet Oxygen by ICG-CPSNPs. Previous studies have used ICG as a photosensitizer for PDT in a variety of *in vitro* cancer models.[19,54−59] These studies have not addressed the drawbacks of free ICG, which include a short plasma half-life, rapid photobleaching, and quenching due to interactions with serum proteins.[40] Moreover, these studies utilize micromolar concentrations of ICG to gain effectiveness. In the present study, ICG-loaded CPSNPs were evaluated as potential photosensitizers for *in vivo* PDT of leukemia. The encapsulation of ICG within CPSNPs has been previously shown to vastly improve its optical properties which allowed for effective *in vivo* tumor imaging.[32,37] The ability of ICG-CPSNPs to produce singlet oxygen needed to be verified in order to extend this technology as a photosensitizer for PDT. This was accomplished utilizing the Singlet Oxygen Sensor Green (SOSG) in a fluorescent microplate assay comparing ICG-CPSNPs to free ICG. 32D-p210-GFP cells were exposed to 8.75 nM ICG or PEGylated ICG-CPSNPs for 1 h, incubated with 10 μM SOSG for 10 min, and then dosed with 0.2 J/cm^2 near-infrared laser light. At a concentration similar to that used in prior imaging studies, PEGylated ICG-CPSNPs were able to generate significantly more singlet oxygen than free ICG (Figure 5). The propagation of the PDT-initiated oxidative "signal" was further analyzed at the level of superoxide with dihydroethidium (DHE) in a fluorescent microplate assay. 32D-p210-GFP cells were exposed to 8.75 nM ICG or PEGylated ICG-CPSNPs for 1 h, incubated with 20 μM DHE for 30 min, and then dosed with 0.2 J/cm^2 near-infrared laser light. As with singlet oxygen, ICG-CPSNPs were able to generate superoxide whereas free ICG did not (Figure 5). These experiments demonstrated that ICG-CPSNPs could be used as photosensitizers for PDT. Furthermore, superoxide generation was also demonstrated, which indicates that the oxidative signal can propagate to another reactive oxygen species.

Evaluation of LSC-Targeted ICG-CPSNP PDT. The efficacy of antileukemia therapeutics is severely limited in a wide variety of cases and is particularly linked to multidrug-resistant cells such as LSCs. In theory, the elimination of LSCs would sensitize leukemia to conventional therapy or even result in remission without further therapy. In this study, murine 32D-p210-GFP CML cells and human AML patient cells were used to show the *in vitro* efficacy, *via* cellular viability assay, of LSC-targeted ICG-CPSNP PDT (Figure 6A−C). PDT using nontargeted ICG-CPSNPs was efficacious in 32D-p210-GFP cells (30% reduction in viability) but not in either of the AML patient samples evaluated. In contrast, PDT utilizing CD117-targeted ICG-CPSNPs exerted a profound antileukemic effect *in vitro* on 32D-p210-GFP cells (51% reduction in viability). Likewise, a robust antileukemic effect was observed *in vitro* with PDT of two AML patient samples utilizing CD96-targeted ICG-CPSNPs (40 and 33% reductions in viability of samples #202 and #370, respectively). Altogether, these results show that targeted therapy, and in particular LSC-targeted therapy, can improve the *in vitro* efficacy of PDT utilizing ICG-loaded CPSNPs. Indeed therapeutic targeting may simply enhance efficacy by delivering more ICG-CPSNP, and certainly CD117-targeted ICG-CPSNPs internalized more effectively than nontargeted ICG-CPSNPs. However, dramatic improvements in therapeutic efficacy argue for a more profound antileukemic effect that can be attributed to targeting LSCs. Additionally, no therapeutic benefit was observed when cells were treated with Ghost-CPSNPs targeted to either CD117 (32D-p210-GFP cells) or CD96 (AML patient cells). This indicated that there was not a

therapeutic benefit attributable to enhanced delivery of CPSNPs alone, even without ICG and a PDT effect.

Total leukemic cell number and LSC number were next evaluated by flow cytometry to show the LSC-specific *in vitro* therapeutic efficacy of CD117-targeted ICG-CPSNP PDT in the 32D-p210-GFP leukemia model. In response to CD117-targeted therapy, the percent of LSCs significantly decreases while untargeted therapy, as well as untargeted Ghost-CPSNPs, increased the percentage of LSCs (Figure 7). These later results are explained as an

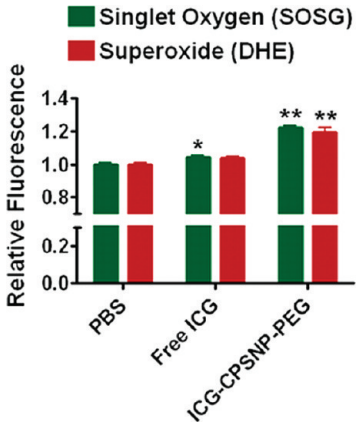

Figure 5. Ability of ICG-CPSNPs to act as photosensitizers for PDT was verified. A fluorescent microplate assay was used to study the generation of singlet oxygen *in vitro* utilizing the Singlet Oxygen Sensor Green (SOSG) (green bars). 32D-p210-GFP cells were exposed to 8.75 nM free ICG or PEGylated ICG-CPSNPs for 1 h, incubated with 10 μM SOSG for 10 min, and then dosed with 0.2 J/cm^2 near-infrared laser light. Propagation of the PDT-initiated oxidative "signal" was further analyzed at the level of superoxide with dihydroethidium (DHE) in a fluorescent microplate assay (red bars). In similar fashion, 32D-p210-GFP cells were exposed to 8.75 nM ICG or PEGylated ICG-CPSNPs for 1 h, incubated with 20 μM DHE for 30 min, and then dosed with 0.2 J/cm^2 near-infrared laser light. ANOVA, *$p < 0.05$ compared to PBS control, **$p < 0.001$ compared to PBS control and free ICG, $n = 12$.

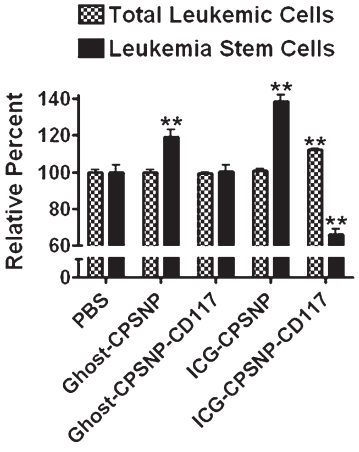

Figure 7. ICG-CPSNP PDT effectively reduces LSCs. Flow cytometry was used to study 32D-p210-GFP cells and their LSC subpopulation (GFP$^+$lineage$^-$CD117$^+$Sca-1$^+$) in response to treatment. Cells were treated with 10 nM ICG-CPSNPs, CD117-targeted ICG-CPSNPs, or equivalent PBS, Ghost-CPSNP, or CD117-targeted Ghost-CPSNP controls, followed 1 h later by 12.5 J/cm^2 near-infrared laser dosage. Cells were allowed to incubate for 24 h before surface marker staining and flow cytometry. GFP$^+$ cells analyzed as total leukemic cells (checkered bars) are graphed as relative percents of the PBS control (4.5×10^6 cells/mL). LSCs (black bars) are graphed as relative percents of the PBS control (0.2% of the total leukemic cellular population). ANOVA, ** $p < 0.05$ relative to the PBS control, $n = 3$.

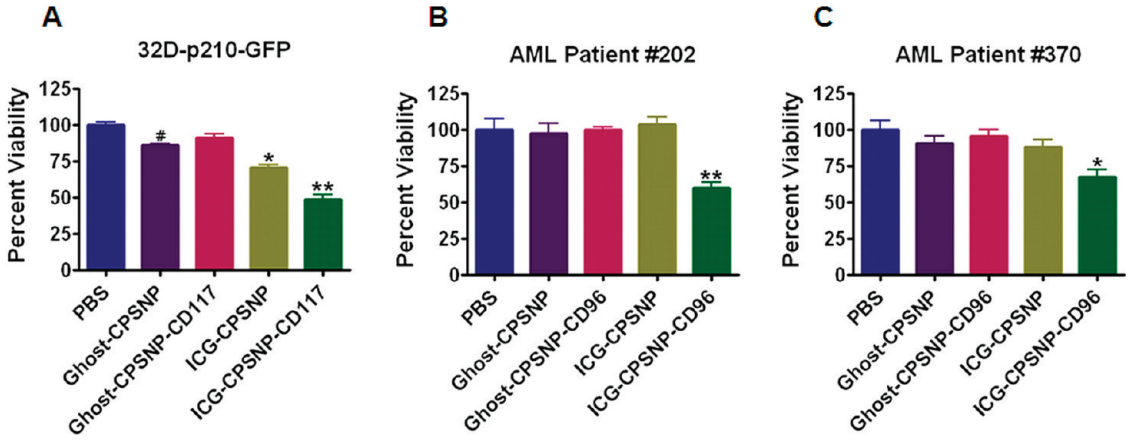

Figure 6. Myeloid leukemia is effectively treated *in vitro* by LSC-targeted ICG-CPSNP PDT. (A) Cellular viability of 32D-p210-GFP chronic myeloid leukemia cells was determined following treatment with 10 nM ICG-CPSNPs, CD117-targeted ICG-CPSNPs, or equivalent PBS, empty (Ghost)-CPSNP, or CD117-targeted Ghost-CPSNP controls, followed 2 h later by 1 J/cm^2 near-infrared laser dosage. Cellular viability was determined 24 h later. ANOVA, #$p < 0.001$ compared to PBS, *$p < 0.001$ compared to PBS, Ghost-CPSNPs, and CD117-targeted Ghost-CPSNPs, **$p < 0.001$ compared to all treatments, $n \geq 12$. (B) Cellular viability of cells from a human acute myeloid leukemia patient (#202) was determined following treatment with 10 nM ICG-CPSNPs, CD96-targeted ICG-CPSNPs, or equivalent PBS, empty (Ghost)-CPSNP, or CD96-targeted Ghost-CPSNP controls, followed 2 h later by 1 J/cm^2 near-infrared laser dosage. Cellular viability was determined 24 h later. ANOVA, **$p < 0.001$ compared to all treatments, $n \geq 9$. (C) Cellular viability following CD96-targeted ICG-CPSNP PDT was evaluated in a similar manner with cells from a second human acute myeloid leukemia patient (#370). ANOVA, *$p < 0.05$ compared to PBS, Ghost-CPSNPs, and CD96-targeted Ghost-CPSNPs, $n \geq 9$.

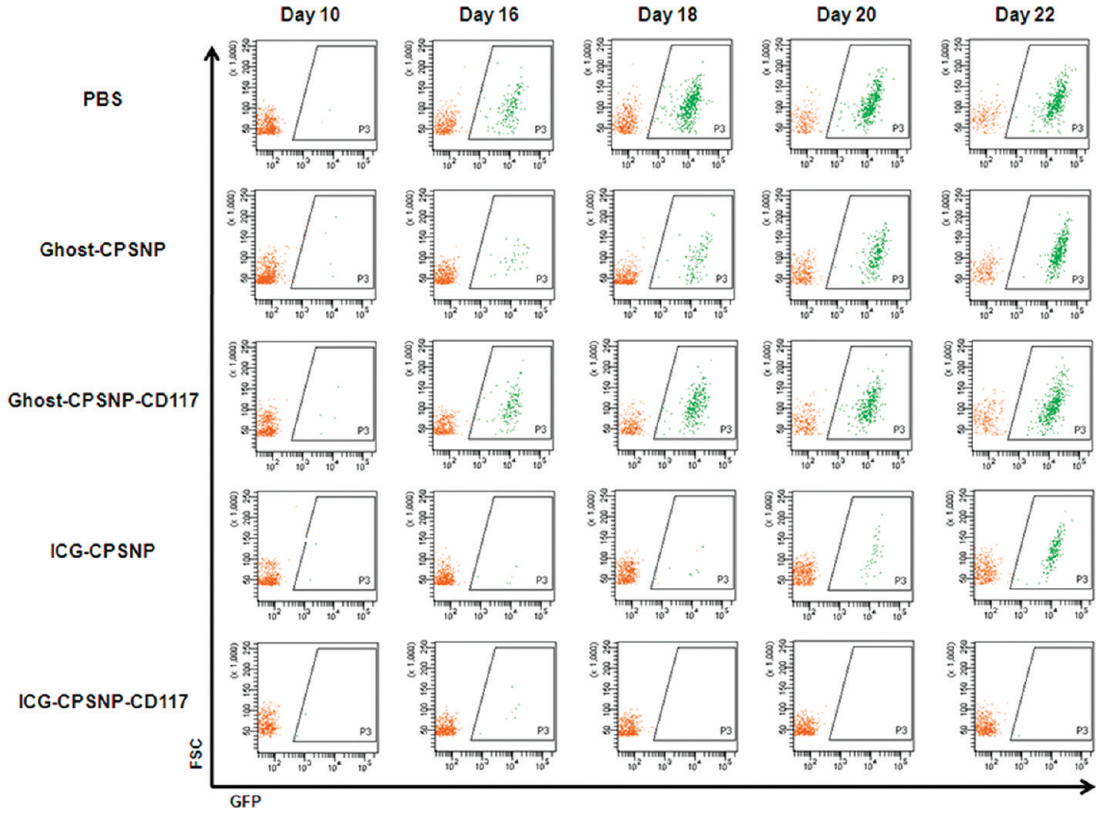

Figure 8. LSC-targeted ICG-CPSNP PDT blocks myeloid leukemia growth *in vivo*. Myeloid leukemia was established in C3H/HeJ mice with 32D-p210-GFP cells, and mice were treated with PBS, empty (Ghost)-CPSNPs, CD117-targeted Ghost-CPSNPs, ICG-CPSNPs, or CD117-targeted ICG- CPSNPs followed by near-infrared laser treatment of the spleen. The leukemia burden was followed by routine flow cytometry analysis of GFP^+ leukemic cells in the peripheral blood (green fluorescence). Representative flow cytometry dot plots (n = 7 per group).

enrichment of the more resistant LSCs by virtue of a lack of LSC targeting. Importantly though, CD117-targeted ICG-CPSNP PDT substantially decreased the LSC population, providing direct evidence for their selective therapeutic elimination. Additionally, CD117-targeted ICG-CPSNP PDT resulted in a significant increase in the total number of leukemic cells (Figure 7). The increase in the total number of leukemic cells is likely a direct result from the decrease in the LSC population.

The observation of an increase in total leukemic cells may seem counterintuitive at first but carries specific meaning in the context of LSC biology. Specifically, it has been suggested that LSCs, like other cancer stem cells, are quiescent and are not cycling.[60,61] This status has been shown to be important to protecting LSCs from conventional DNA-damaging chemotherapeutic agents.[60,61] Recent studies also showed that disruption of the cell cycle inhibitor p21 caused LSCs to enter the cell cycle and hyper-proliferate causing dramatic depletion of the LSC population.[61] More importantly, these studies showed that p21-deficient cells were unable to induce leukemia in immunodeficient hosts despite the presence of a leukemogenic oncogene.[61] This experiment is typically used to define cancer stem cells, and so the inability of nonquiescent p21-deficient LSC-like cells to initiate leukemia showed they were not functional LSCs. These studies not only demonstrated an important aspect of LSC biology but also provided support for the idea of a two-step approach to leukemia treatment involving an initial LSC-targeted approach exploiting LSC biology followed by a more general antileukemia therapy. In the context of the present study, it is likely that CD117-targeted ICG-CPSNP PDT selectively decreased LSCs and caused a transient proliferation of "normal" leukemia cells that were further unable to maintain the viability of the leukemia as a whole. This proliferative event of non-LSCs is not thought of as a clinical problem because these cells are readily treated by first-line antiproliferative chemotherapeutics. The challenge to conventional therapy is LSCs that evade conventional therapies and contribute to relapse and multidrug resistance. Therefore, targeting CD117 on LSCs of CML, or CD96 on LSCs of AML, offers a distinct therapeutic advantage to destroy the particular cells responsible for leukemia development, maintenance, progression, relapse, and resistance. Additionally, it is practical

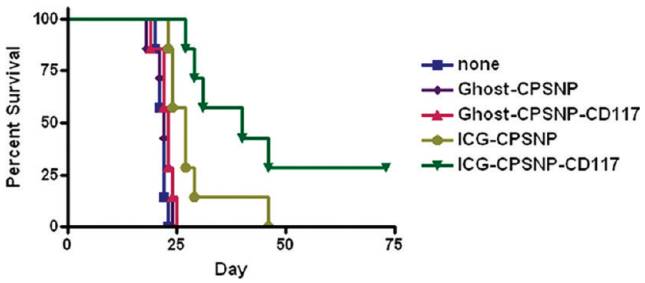

Figure 9. LSC-targeted ICG-CPSNP PDT extended the life span of leukemic mice. Myeloid leukemia was established in C3H/HeJ mice with 32D-p210-GFP cells, and mice were treated with PBS, empty (Ghost)-CPSNPs, CD117-targeted Ghost-CPSNPs, ICG-CPSNPs, or CD117-targeted ICG-CPSNPs followed by near-infrared laser treatment of the spleen. Survival of leukemic C3H/HeJ mice was monitored. A logrank test indicated significance ($p < 0.05$) between the curves ($n = 7$ per group).

to suggest that LSC-targeted ICG-CPSNP PDT could be used as the first step in a multistep therapeutic approach to the treatment of leukemia.

***In Vivo* Efficacy of LSC-Targeted ICG-CPSNP PDT.** The development of CPSNPs allowed for improved optical properties of encapsulated dyes, as well as for protection of therapeutics during systemic delivery.[32−35] Encapsulation of the near-infrared fluoroprobe ICG within CPSNPs vastly improved its optical properties, which allowed for effective deep-tissue tumor imaging.[32,37] This optical improvement further suggested that ICG-CPSNPs could be effectively used as photosensitizers for PDT, which was confirmed by *in vitro* studies indicating an ability to generate singlet oxygen and to reduce leukemia viability (Figures 5 and 6). Enhanced efficacy was observed by specifically targeting ICG-CPSNPs to surface features expressed on LSCs. In addition to depleting the cellular population responsible for the leukemia, targeting most likely caused the ICG-CPSNPs to enter the cells *via* receptor-mediated endocytosis rather than pinocytosis. This different manner of entering cells likely improved the lifetime of the ICG-CPSNP by further delaying or preventing its trafficking to lysosomes where the acidic pH would cause its dissolution. The potential *in vivo* efficacy of PDT utilizing ICG-CPSNPs was speculated to be relative to the amount of nanoparticle endocytosed by cancerous cells. In the case of leukemia, it was hypothesized that minimal *in vivo* PDT efficacy would be achieved, as ICG-CPSNPs would not accumulate *via* enhanced permeation and retention like they were shown to in solid tumors[32,37] However, selective targeting of ICG-CPSNPs was predicted to yield effective *in vivo* PDT of leukemia. Moreover, selective targeting to LSCs was foreseen to enhance *in vivo* PDT by selectively targeting the cellular population responsible for the maintenance and progression of the disease.

To further evaluate ICG-CPSNP PDT, an *in vivo* 32D-p210-GFP leukemia model was employed. This model was advantageous as it induced a leukemia that developed in a predictable manner, with distinct GFP^+ populations of leukemic cells in the blood which were measurable by flow cytometry (green fluorescence).[42,43] Furthermore, as previously mentioned, the 32Dp210-GFP CML model behaves like AML *in vivo* with its rapid onset and proliferation of immature leukemic blasts.[2,43] LSC-targeted ICG-CPSNP PDT, initiated by systemic injection of CPSNPs followed by near-infrared-irradiation of the spleen, evoked a robust antileukemic effect evident by the absence of GFP^+ leukemic cells in the blood (Figure 8). This blockade of leukemic cell proliferation *in vivo* correlated with a profound and dramatic extension in survival (Figure 9). Some animals within the group that received CD117-targeted ICG-CPSNP PDT had no evidence of leukemia and rather exhibited leukemia-free survival. All animals in other experimental groups eventually succumbed to their disease. Importantly, animals receiving CD117-targeted CPSNPs without ICG did not show therapeutic benefit, indicating that simple CD117 targeting was not sufficient and that ICG-mediated PDT was a therapeutic requirement. Potential toxicity of CD117-targeted ICG-CPSNP PDT was also evaluated. Normal hematopoietic cells were possible targets for side effects given the prevalence of CD117 on hematopoietic progenitors.[62,63] Flow cytometry light scattering analysis of peripheral blood showed a minor degree of myelosuppression in response to CD117-targeted ICG-CPSNP PDT (Figure 10A, blue arrows). This was revealed as a minor depletion of a normal myeloid population. This indication of myelosuppression varied during the course of the trial but never resulted in a complete loss of this normal cellular population. Finally, healthy athymic nude mice were injected with a 2X dose of CD117-targeted ICG-CPSNPs to evaluate targeting of normal tissues. Athymic nude mice were chosen for this study because they are hairless. Only the spleen was visualized by bioimaging one day following injection of CD117-targeted ICG-CPSNPs (Figure 10B). Targeting the spleen was not unexpected as many of the normal cells residing in the spleen are $CD117^+$.[62,63] Reversible and negligible off-target toxicity is an

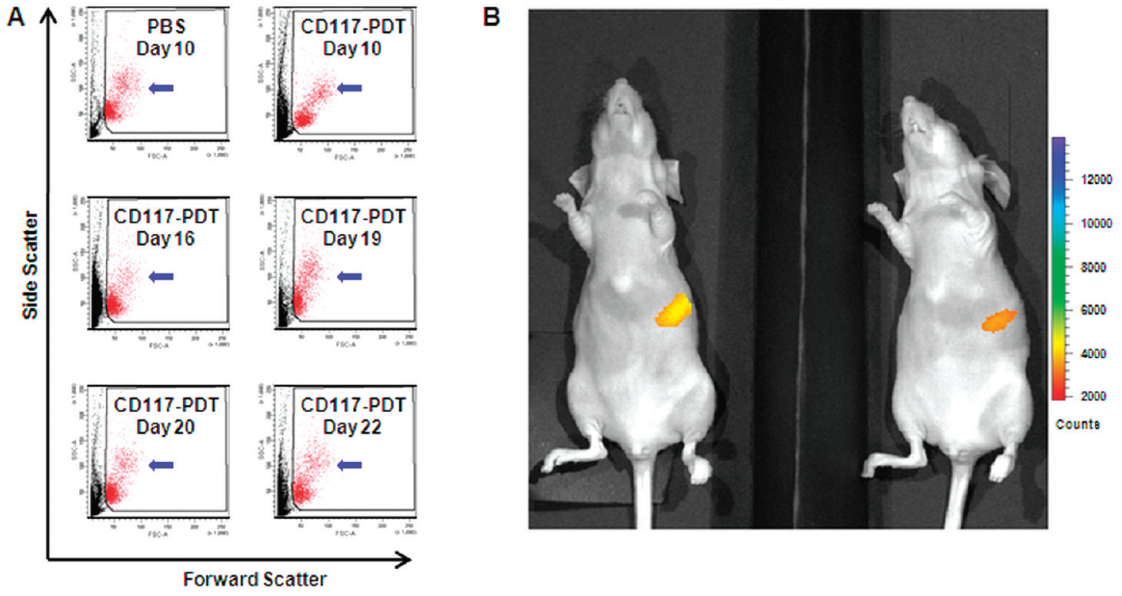

Figure 10. Potential off-target toxicity of CD117-targeted ICG-CPSNP PDT was evaluated. (A) Flow cytometry light scattering analysis of peripheral blood showed a minor degree of myelosuppression in response to CD117-targeted ICG-CPSNP PDT (blue arrows). This was revealed as a minor depletion of a normal myeloid population. (B) Healthy athymic nude mice were injected with a 2X dose of CD117-targeted ICG-CPSNPs to evaluate targeting of normal tissues. Athymic nude mice were chosen for this study because they are hairless. The spleen was visualized by bioimaging one day following injection of CD117-targeted ICG-CPSNPs.

acceptable outcome of LSC-targeted therapies. Leukemia can eventually overcome untargeted ICG-CPSNP PDT due to the fact that LSCs, the specific leukemic cell population responsible for therapy resistance, are not eliminated. In this study, the profound efficacy observed with PDT utilizing CD117-targeted ICG-CPSNPs, including leukemia-free survival in some animals, argued that LSCs were successfully targeted and eliminated.

CONCLUSIONS

PDT has been utilized as an alternative to conventional anticancer therapies. Unfortunately, PDT is limited to the treatment of a small subset of easily accessible cancers due to limitations of light to penetrate tissue and is further limited by inefficient and toxic photosensitizers. PDT is not currently used for the direct treatment of leukemia. However, recent studies have focused on its potential utility to purge autologous hematopoietic stem cell transplants of leukemic cells *ex vivo* in a manner dependent on differential passive uptake of photosensitizers compared with normal hematopoietic cells.[30] In the present study, PDT utilizing ICG-loaded CPSNPs was evaluated in models of leukemia. The advantage of CPSNP-encapsulated ICG lies in the superior optical properties once encapsulated yielding a product that can perform as an optimal photosensitizer even at considerable tissue depth.[32,37] The biocompatibility of both CPSNPs and ICG, as well as the stability of CPSNPs at physiological pH, lends an added dimension of benefit in the form of reduced off-target toxicity. CPSNPs targeting LSCs were developed and employed to improve PDT of leukemia using ICG-CPSNPs. General targeting of CPSNPs was anticipated to have a beneficial effect as this would maximize the amount of therapeutic delivered to leukemic cells. Similarly, in previous studies of solid tumor models targeting enhanced the accumulation of CPSNPs. However, as a malignancy of nonadherent cells, leukemia presented a great therapeutic challenge owing to a lack of enhanced permeation and retention of PEGylated CPSNPs. More so, the expansiveness of leukemia as a hematological malignancy, involving potentially both blood and bone marrow, presented an even greater hurdle that demanded selective targeting to the cellular populations responsible for the development, progression, multidrug resistance, and relapse of the disease. For these reasons, ICG-CPSNPs were targeted to surface features found on LSCs, the specific cells thought to be responsible for the development and progression of the leukemia, as well as the inherent ability of leukemia to resistant treatment and to relapse. By targeting LSCs, in an *in vivo* model of CML, as well as in human AML patient samples, PDT utilizing ICG-CPSNPs became extremely effective. More so, LSC-targeted therapy resulted in some mice exhibiting leukemia-free survival, indicative of successful LSC eradication. Altogether, PDT utilizing LSC-targeted ICG-CPSNPs is a highly efficacious therapeutic option for the treatment of leukemia. The ability to eliminate LSCs by PDT utilizing targeted ICG-CPSNPs,

a nanotherapy with minimal side effects, offers a dramatic improvement for the treatment of leukemia, an aggressive cancer which includes a profound pediatric disparity.

MATERIALS AND METHODS

Reagents. Cell culture medium was purchased from Mediatech (Manassas, VA); FBS was obtained from Gemini Bio-Products (West Sacramento, CA), and other cell culture reagents were from Invitrogen (Carlsbad, CA). Antibodies were from eBiosciences (San Diego, CA), BD Biosciences (San Jose, CA), Miltenyi Biotech (Bergisch Gladbach, Germany), and Santa Cruz Biotechnology (Santa Cruz, CA). EDAC and Sulfo-NHS were from Pierce (Thermo Fisher Scientific, Rockford, IL). ICG was from TCI America (Portland, OR). Cascade Blue and Singlet Oxygen Sensor Green (SOSG) was from Invitrogen. Dihydroethidium (DHE) was from EMD Biosciences (San Diego, CA). PEG compounds were from JenKem Technology (Allen, TX). Unless specified otherwise, other reagents were from Sigma (St. Louis, MO).

Cell Culture. Murine 32D-p210-GFP CML cells and human AML patient cells were cultured in RPMI-1640 supplemented with 10% FBS and antibiotic−antimycotic solution. All cultures were maintained at 37 °C and 5% CO_2. 32D-p210-GFP cells were originally obtained from the laboratory of Dr. Ralph Arlinghaus from the Department of Molecular Pathology at the University of Texas MD Anderson Cancer Center.[43] The 32D-p210-GFP cell line was created from the 32D cell line originally derived from C3H/HeJ mice,[64] which was later transduced with the *Bcr-Abl* oncogene (p210)[65] and last with GFP.[42] AML patient cells were obtained with informed consent, which was approved by the Pennsylvania State University Institutional Review Board.

Animal Models. Myeloid leukemia was established and monitored in C3H/HeJ mice, as previously described.[42,43] Briefly, female C3H/HeJ mice (7−9 weeks old) were obtained from the Jackson Laboratory (Bar Harbor, ME), and leukemia was initiated by tail vein injection of 2×10^6 32D-p210-GFP cells. Therapeutic trials commenced 3−5 days after cell injection, once GFP^+ cells were detectable in the peripheral blood. For therapeutic trials, leukemic mice received 0.1 mL injections of ICG-CPSNPs diluted approximately 1:10 into PBS (200 nM preinjection concentration of ICG), or controls, followed within 30 min by 12.5 J/cm^2 near-infrared laser irradiation directed at the spleen. Treatments occurred once every three days. Leukemia burden was monitored by collecting a small aliquot of blood (tail prick) into red blood cell lysis buffer and by analyzing GFP^+ cells *via* flow cytometry. Each treatment group consisted of seven mice. Bioimaging of normal tissue targeting by CD117-targeted ICG-CPSNPs was performed as previously described.[32,37] Briefly, female athymic nude mice (4 weeks old) were obtained from Harlan (Indianapolis, IN) and injected with 0.1 mL of CD117-targeted ICG-CPSNPs diluted approximately 1:5 into PBS (200 nM preinjection concentration of ICG). One day following injections, near-infrared bioimaging was performed using a Xenogen IVIS 50 animal imaging system (Caliper Life Sciences, Hopkinton, MA). All animal procedures were approved by the Pennsylvania State University College of Medicine Institutional Animal Care and Use Committee.

CPSNP Bioconjugation and Physical Characterization. CPSNPs loaded with ICG, or cascade blue, were prepared as previously described.[32−35,37] EDAC (250 μL at 0.2 mg/mL in CO_2-free deionized water) was added to citrate-terminated CPSNPs dispersed in 3 mL of 70/30 ethanol/water. After 5 min, sulfo-NHS (250 μL at 0.2 mg/mL in CO_2-free deionized water) was added to the solution, and after another 5 min, methoxy-PEG-amine (250 μL at 2 μg/mL in CO_2-free deionized water) and carboxy-PEG-amine (50 μL at 0.6 μg/mL in CO_2-free deionized water) were added simultaneously. The nanoparticles were reacted for 15 h at 50 °C while stirring. The carboxy terminal group of the carboxy-PEG-amine was used to conjugate antibodies to the PEG surface of the CPSNPs. EDAC (250 μL at 12 μg/mL in CO_2-free deionized water) was added to carboxy-PEGylated CPSNPs while stirring at room temperature. After 5 min, sulfo-NHS (250 μL at 16 μg/mL in CO_2-free deionized water) was added to the solution, and the antibody solutions were added after 5 min. For bioconjugation, a molar excess of antibody (to carboxy-PEG) was added to the nanoparticle solution. Size distributions for Ghost-CPSNPs or Cascade Blue-loaded CPSNPs were obtained through dynamic light scattering (DLS) using a Malvern Instruments Nano-S Zetasizer (Malvern, Worcestershire, United Kingdom). To verify size, transmission electron microscopy (TEM) was performed on dried nanoparticles, prepared on a carbon grid with a copper backing, using a JEOL JEM 1200 EXII instrument. Zeta potential distributions for Ghost-CPSNPs or Cascade Blue-loaded CPSNPs were obtained using a Brookhaven Instruments ZetaPALS zeta potential analyzer (Holtsville, NY).

CPSNP Internalization. Cascade Blue-loaded CPSNPs were added to a 96-well microplate with cultured 32D-p210-GFP cells (5×10^3 cells per well) or to wells with only culture media. Fluorescence was routinely evaluated by exciting at 405 nm and measuring emission at 450 nm with a Molecular Devices SpectraMax Gemini XS fluorescence microplate reader (Sunnyvale, CA). The loss of fluorescence in the presence of cells, minus the loss without cells (background), was used to quantify internalization of the Cascade Blue-loaded CPSNPs. Internalization was graphed using the equation: CPSNP internalization = $\log_{10}$(1/fluorescence).

Flow Cytometry. Cells were washed and resuspended in PBS with mouse BD Fc Block (BD Biosciences) or human FcR blocking reagent (Miltenyi Biotech) (1 μg per 1×10^6 splenocytes) and incubated for 15 min at 4 °C. Antibodies targeting human CD34 (FITC-conjugated), human CD38 (Alexa Fluor 700-conjugated), human CD96 (PE-conjugated), mouse CD117 (Alexa Fluor 700- or V450-conjugated), mouse Sca-1 (PerCP-Cy5.5-conjugated), or a mouse lineage cocktail (APC-conjugated targeting CD3ε, CD11b, CD45R/B220, Ly-76, and Gr-1) were added. Cells were incubated for 15 min at 4 °C with various combinations of the antibodies (1 μg per 1×10^6 cells). Multicolor flow cytometry was performed at the Pennsylvania State University College of Medicine Flow Cytometry Core Facility utilizing a BD Biosciences LSR II Special Order flow cytometer. BD FACS Diva software and FlowJo software (Tree Star, Inc., Ashland, OR) were used to analyze results.

Reactive Oxygen Species Detection. 32D-p210-GFP cells were plated at 1×10^4 cells per well in 96-well tissue culture plates. Cells were treated with 8.75 nM free ICG or 8.75 nM PEGylated ICG-CPSNPs for 1 h prior to incubation in the dark with 10 μM SOSG (10 min) or 20 μM DHE (30 min) followed by 0.2 J/cm^2 near-infrared laser light dosage. SOSG was used to detect singlet oxygen generation *in vitro* as described by Flors *et al.*[66] DHE was used to detect superoxide generation *in vitro* as previously described.[67] A fluorescent microplate reader was used to detect SOSG (excitation at 485 nm and emission at 525 nm) and DHE (excitation at 485 nm and emission at 600 nm).

Cell Viability. 32D-p210-GFP cells, or two separate AML patient cellular samples, were plated at 5×10^3 cells per well in 96-well tissue culture plates. Cells were then pretreated for 2 h in media containing CPSNPs (10 nM concentration of ICG) and then given near-infrared laser light (1 J/cm^2). Twenty-four hours following treatment, cellular viability was assessed using a Cell Titer 96 AQ_{ueous} nonradioactive cell proliferation assay according to the manufacturer's instructions (Promega, Madison, WI). Viability was determined by measuring absorbance at 490 nm using a microplate reader and normalized to the viability observed under control conditions. Results were determined from at least nine independent experiments.

Statistical Analysis. GraphPad Prism 5.0 software was used to plot graphs as well as to determine significance of results. ANOVA, followed by Bonferroni comparison, was used to

determine significance between treatment groups. To determine significance of survival, a logrank test was used. All data represent averages ± standard error of the mean.

Acknowledgment. This study was funded by a Children's Miracle Network grant to B.M.B. The Penn State Research Foundation has licensed CPSNPs to Keystone Nano, Inc. (State College, PA) for commercialization. J.H.A. and M.K. serve as CSO and CMO of Keystone Nano, Inc., respectively.

REFERENCES AND NOTES

1. Radhi, M.; Meshinchi, S.; Gamis, A. Prognostic Factors in Pediatric Acute Myeloid Leukemia. *Curr. Hematol. Malig Rep.* **2010**, *5*, 200–206.
2. Perrotti, D.; Jamieson, C.; Goldman, J.; Skorski, T. Chronic Myeloid Leukemia: Mechanisms of Blastic Transformation. *J. Clin. Invest.* **2010**, *120*, 2254–2264.
3. Sloma, I.; Jiang, X.; Eaves, A. C.; Eaves, C. J. Insights Into the Stem Cells of Chronic Myeloid Leukemia. *Leukemia* **2010**, *24*, 1823–1833.
4. Roboz, G. J.; Guzman, M. Acute Myeloid Leukemia Stem Cells: Seek and Destroy. *Expert Rev. Hematol.* **2009**, *2*, 663–672.
5. Perl, A.; Carroll, M. BCR-ABL Kinase Is Dead; Long Live the CML Stem Cell. *J. Clin. Invest.* **2011**, *121*, 22–25.
6. Misaghian, N.; Ligresti, G.; Steelman, L. S.; Bertrand, F. E.; Basecke, J.; Libra, M.; Nicoletti, F.; Stivala, F.; Milella, M.; Tafuri, A.; *et al.* Targeting the Leukemic Stem Cell: The Holy Grail of Leukemia Therapy. *Leukemia* **2009**, *23*, 25–42.
7. Hosen, N.; Park, C. Y.; Tatsumi, N.; Oji, Y.; Sugiyama, H.; Gramatzki, M.; Krensky, A. M.; Weissman, I. L. CD96 Is a Leukemic Stem Cell-Specific Marker in Human Acute Myeloid Leukemia. *Proc. Natl. Acad. Sci. U.S.A.* **2007**, *104*, 11008–11013.
8. Chen, Y.; Hu, Y.; Zhang, H.; Peng, C.; Li, S. Loss of the Alox5 Gene Impairs Leukemia Stem Cells and Prevents Chronic Myeloid Leukemia. *Nat. Genet.* **2009**, *41*, 783–792.
9. Gerber, J. M.; Qin, L.; Kowalski, J.; Smith, B. D.; Griffin, C. A.; Vala, M. S.; Collector, M. I.; Perkins, B.; Zahurak, M.; Matsui, W.; *et al.* Characterization of Chronic Myeloid Leukemia Stem Cells. *Am. J. Hematol.* **2011**, *86*, 31–37.
10. Robertson, C. A.; Evans, D. H.; Abrahamse, H. Photodynamic Therapy (PDT): A Short Review on Cellular Mechanisms and Cancer Research Applications for PDT. *J. Photochem. Photobiol. B* **2009**, *96*, 1–8.
11. Dolmans, D. E.; Fukumura, D.; Jain, R. K. Photodynamic Therapy for Cancer. *Nat. Rev. Cancer* **2003**, *3*, 380–387.
12. Juarranz, A.; Jaen, P.; Sanz-Rodriguez, F.; Cuevas, J.; Gonzalez, S. Photodynamic Therapy of Cancer. Basic Principles and Applications. *Clin. Transl. Oncol.* **2008**, *10*, 148–154.
13. Ortel, B.; Shea, C. R.; Calzavara-Pinton, P. Molecular Mechanisms of Photodynamic Therapy. *Front. Biosci.* **2009**, *14*, 4157–4172.
14. Wainwright, M. Photodynamic Therapy: the Development of New Photosensitisers. *Anticancer Agents Med. Chem.* **2008**, *8*, 280–291.
15. Sibani, S. A.; McCarron, P. A.; Woolfson, A. D.; Donnelly, R. F. Photosensitiser Delivery for Photodynamic Therapy. Part 2: Systemic Carrier Platforms. *Expert Opin. Drug Delivery* **2008**, *5*, 1241–1254.
16. Huang, Z.; Xu, H.; Meyers, A. D.; Musani, A. I.; Wang, L.; Tagg, R.; Barqawi, A. B.; Chen, Y. K. Photodynamic Therapy for Treatment of Solid Tumors—Potential and Technical Challenges. *Technol. Cancer. Res. Treat.* **2008**, *7*, 309–320.
17. Chatterjee, D. K.; Fong, L. S.; Zhang, Y. Nanoparticles in Photodynamic Therapy: An Emerging Paradigm. *Adv. Drug Delivery Rev.* **2008**, *60*, 1627–1637.
18. Reddy, G. R.; Bhojani, M. S.; McConville, P.; Moody, J.; Moffat, B. A.; Hall, D. E.; Kim, G.; Koo, Y. E.; Woolliscroft, M. J.; Sugai, J. V.; *et al.* Vascular Targeted Nanoparticles for Imaging and Treatment of Brain Tumors. *Clin. Cancer Res.* **2006**, *12*, 6677–6686.
19. Rungta, P.; Bandera, Y. P.; Roeder, R. D.; Li, Y.; Baldwin, W. S.; Sharma, D.; Sehorn, M. G.; Luzinov, I.; Foulger, S. H. Selective Imaging and Killing of Cancer Cells with Protein-Activated Near-Infrared Fluorescing Nanoparticles. *Macromol. Biosci.* **2011**, *11*, 927−933.
20. Qin, M.; Hah, H. J.; Kim, G.; Nie, G.; Lee, Y. E.; Kopelman, R. Methylene Blue Covalently Loaded Polyacrylamide Nanoparticles for Enhanced Tumor-Targeted Photodynamic Therapy. *Photochem. Photobiol. Sci.* **2011**, *10*, 832–841.
21. Ohulchanskyy, T. Y.; Roy, I.; Goswami, L. N.; Chen, Y.; Bergey, E. J.; Pandey, R. K.; Oseroff, A. R.; Prasad, P. N. Organically Modified Silica Nanoparticles with Covalently Incorporated Photosensitizer for Photodynamic Therapy of Cancer. *Nano Lett.* **2007**, *7*, 2835–2842.
22. Lee, Y. E.; Kopelman, R. Polymeric Nanoparticles for Photodynamic Therapy. *Methods Mol. Biol.* **2011**, *726*, 151–178.
23. Lee, S. J.; Koo, H.; Jeong, H.; Huh, M. S.; Choi, Y.; Jeong, S. Y.; Byun, Y.; Choi, K.; Kim, K.; Kwon, I. C. Comparative Study of Photosensitizer Loaded and Conjugated Glycol Chitosan Nanoparticles for Cancer Therapy. *J. Controlled Release* **2011**, *152*, 21−29.
24. Hocine, O.; Gary-Bobo, M.; Brevet, D.; Maynadier, M.; Fontanel, S.; Raehm, L.; Richeter, S.; Loock, B.; Couleaud, P.; Frochot, C.; *et al.* Silicalites and Mesoporous Silica Nanoparticles for Photodynamic Therapy. *Int. J. Pharm.* **2010**, *402*, 221–230.
25. Cheng, Y.; Meyers, J. D.; Broome, A. M.; Kenney, M. E.; Basilion, J. P.; Burda, C. Deep Penetration of a PDT Drug into Tumors by Noncovalent Drug−Gold Nanoparticle Conjugates. *J. Am. Chem. Soc.* **2011**, *133*, 2583–2591.
26. Feuerstein, T.; Schauder, A.; Malik, Z. Silencing of ALA Dehydratase Affects ALA-Photodynamic Therapy Efficacy in K562 Erythroleukemic Cells. *Photochem. Photobiol. Sci.* **2009**, *8*, 1461–1466.
27. Furre, I. E.; Shahzidi, S.; Luksiene, Z.; Moller, M. T.; Borgen, E.; Morgan, J.; Tkacz-Stachowska, K.; Nesland, J. M.; Peng, Q. Targeting PBR by Hexaminolevulinate-Mediated Photodynamic Therapy Induces Apoptosis through Translocation of Apoptosis-Inducing Factor in Human Leukemia Cells. *Cancer Res.* **2005**, *65*, 11051–11060.
28. Gamaleia, N. F.; Shishko, E. D.; Gluzman, D. F.; Sklyarenko, L. M. Sensitivity of Normal and Malignant Human Lymphocytes to 5-Aminolevulinic Acid-Mediated Photodynamic Damage. *Exp. Oncol.* **2008**, *30*, 65–69.
29. Pluskalova, M.; Peslova, G.; Grebenova, D.; Halada, P.; Hrkal, Z. Photodynamic Treatment (ALA-PDT) Suppresses the Expression of the Oncogenic Bcr-Abl Kinase and Affects the Cytoskeleton Organization in K562 Cells. *J. Photochem. Photobiol. B* **2006**, *83*, 205–212.
30. Huang, H. F.; Chen, Y. Z.; Wu, Y.; Chen, P. Purging of Murine Erythroblastic Leukemia by ZnPcS2P2-Based-Photodynamic Therapy. *Bone Marrow Transplant.* **2006**, *37*, 213–217.
31. Maeda, H. The Enhanced Permeability and Retention (EPR) Effect in Tumor Vasculature: the Key Role of Tumor-Selective Macromolecular Drug Targeting. *Adv. Enzyme Regul.* **2001**, *41*, 189–207.
32. Altınoğlu, E. İ.; Russin, T. J.; Kaiser, J. M.; Barth, B. M.; Eklund, P. C.; Kester, M.; Adair, J. H. Near-nfrared Emitting Fluorophore-Doped Calcium Phosphate Nanoparticles for *In Vivo* Imaging of Human Breast Cancer. *ACS Nano* **2008**, *2*, 2075–2084.
33. Kester, M.; Heakal, Y.; Fox, T.; Sharma, A.; Robertson, G. P.; Morgan, T. T.; Altinoglu, E. I.; Tabakovic, A.; Parette, M. R.; Rouse, S. M.; *et al.* Calcium Phosphate Nanocomposite Particles for *In Vitro* Imaging and Encapsulated Chemotherapeutic Drug Delivery to Cancer Cells. *Nano Lett.* **2008**, *8*, 4116–4121.
34. Morgan, T. T.; Muddana, H. S.; Altinoglu, E. I.; Rouse, S. M.; Tabakovic, A.; Tabouillot, T.; Russin, T. J.; Shanmugavelandy, S. S.; Butler, P. J.; Eklund, P. C.; *et al.* Encapsulation of Organic Molecules in Calcium Phosphate Nanocomposite Particles for Intracellular Imaging and Drug Delivery. *Nano Lett.* **2008**, *8*, 4108–4115.
35. Muddana, H. S.; Morgan, T. T.; Adair, J. H.; Butler, P. J. Photophysics of Cy3-Encapsulated Calcium Phosphate Nanoparticles. *Nano Lett.* **2009**, *9*, 1559–1566.

36. Graham, F. L.; van der Eb, A. J. A New Technique for the Assay of Infectivity of Human Adenovirus 5 DNA. *Virology* **1973**, *52*, 456–467.
37. Barth, B. M.; Sharma, R.; Altinoglu, E. I.; Morgan, T. T.; Shanmugavelandy, S. S.; Kaiser, J. M.; McGovern, C.; Matters, G. L.; Smith, J. P.; Kester, M.; *et al.* Bioconjugation of Calcium Phosphosilicate Composite Nanoparticles for Selective Targeting of Human Breast and Pancreatic Cancers *In Vivo*. *ACS Nano* **2010**, *4*, 1279–1287.
38. Russin, T. J.; Altinoglu, E. I.; Adair, J. H.; Eklund, P. C. Measuring the Fluorescent Quantum Efficiency of Indocyanine Green Encapsulated in Nanocomposite Particulates. *J. Phys.: Condens. Matter* **2010**, *22*, 334217.
39. Bennett, T. J.; Barry, C. J. Ophthalmic Imaging Today: An Ophthalmic Photographer's Viewpoint—A Review. *Clin. Experiment. Ophthalmol.* **2009**, *37*, 2–13.
40. Desmettre, T.; Devoisselle, J. M.; Mordon, S. Fluorescence Properties and Metabolic Features of Indocyanine Green (ICG) as Related to Angiography. *Surv. Ophthalmol.* **2000**, *45*, 15–27.
41. Ozpolat, B.; Sood, A. K.; Lopez-Berestein, G. Nanomedicine Based Approaches for the Delivery of siRNA in Cancer. *J. Intern. Med.* **2010**, *267*, 44–53.
42. Ling, X.; Wang, Y.; Dietrich, M. F.; Andreeff, M.; Arlinghaus, R. B. Vaccination with Leukemia Cells Expressing Cell-Surface-Associated GM-CSF Blocks Leukemia Induction in Immunocompetent Mice. *Oncogene* **2006**, *25*, 4483–4490.
43. Keasey, N.; Herse, Z.; Chang, S.; Liggitt, D. H.; Lay, M.; Fairman, J.; Claxton, D. F. A Non-coding Cationic Lipid DNA Complex Produces Lasting Anti-leukemic Effects. *Cancer Biol. Ther.* **2010**, *10*, 625–631.
44. Bathori, G.; Cervenak, L.; Karadi, I. Caveolae—An Alternative Endocytotic Pathway for Targeted Drug Delivery. *Crit. Rev. Ther. Drug Carrier Syst.* **2004**, *21*, 67–95.
45. Hoeller, D.; Volarevic, S.; Dikic, I. Compartmentalization of Growth Factor Receptor Signalling. *Curr. Opin. Cell Biol.* **2005**, *17*, 107–111.
46. Miaczynska, M.; Pelkmans, L.; Zerial, M. Not Just a Sink: Endosomes in Control of Signal Transduction. *Curr. Opin. Cell Biol.* **2004**, *16*, 400–406.
47. Steinman, R. M.; Mellman, I. S.; Muller, W. A.; Cohn, Z. A. Endocytosis and the Recycling of Plasma Membrane. *J. Cell Biol.* **1983**, *96*, 1–27.
48. Broudy, V. C.; Lin, N. L.; Liles, W. C.; Corey, S. J.; O'Laughlin, B.; Mou, S.; Linnekin, D. Signaling *via* Src Family Kinases Is Required for Normal Internalization of the Receptor C-Kit. *Blood* **1999**, *94*, 1979–1986.
49. Chen, Y.; Peng, C.; Sullivan, C.; Li, D.; Li, S. Critical Molecular Pathways in Cancer Stem Cells of Chronic Myeloid Leukemia. *Leukemia* **2010**, *24*, 1545–1554.
50. Hu, Y.; Swerdlow, S.; Duffy, T. M.; Weinmann, R.; Lee, F. Y.; Li, S. Targeting Multiple Kinase Pathways in Leukemic Progenitors and Stem Cells Is Essential for Improved Treatment of Ph+ Leukemia in Mice. *Proc. Natl. Acad. Sci. U.S.A.* **2006**, *103*, 16870–16875.
51. Jahn, T.; Seipel, P.; Coutinho, S.; Urschel, S.; Schwarz, K.; Miething, C.; Serve, H.; Peschel, C.; Duyster, J. Analysing C-Kit Internalization Using a Functional C-Kit-EGFP Chimera Containing the Fluorochrome within the Extracellular Domain. *Oncogene* **2002**, *21*, 4508–4520.
52. Altuna, X.; Lopez, J. P.; Yu, M. A.; Arandazi, M. J.; Harris, J. P.; Wang-Rodriguez, J.; An, Y.; Dobrow, R.; Doherty, J. K.; Ongkeko, W. M. Potential Role of Imatinib Mesylate (Gleevec, STI-571) in the Treatment of Vestibular Schwannoma. *Otol. Neurotol.* **2011**, *32*, 163–170.
53. Babina, M.; Rex, C.; Guhl, S.; Thienemann, F.; Artuc, M.; Henz, B. M.; Zuberbier, T. Baseline and Stimulated Turnover of Cell Surface C-Kit Expression in Different Types of Human Mast Cells. *Exp. Dermatol.* **2006**, *15*, 530–537.
54. Baumler, W.; Abels, C.; Karrer, S.; Weiss, T.; Messmann, H.; Landthaler, M.; Szeimies, R. M. Photo-oxidative Killing of Human Colonic Cancer Cells Using Indocyanine Green and Infrared Light. *Br. J. Cancer* **1999**, *80*, 360–363.
55. Bozkulak, O.; Yamaci, R. F.; Tabakoglu, O.; Gulsoy, M. Photo-Toxic Effects of 809-nm Diode Laser and Indocyanine Green on MDA-MB231 Breast Cancer Cells. *Photodiagn. Photodyn. Ther.* **2009**, *6*, 117–121.
56. Crescenzi, E.; Varriale, L.; Iovino, M.; Chiaviello, A.; Veneziani, B. M.; Palumbo, G. Photodynamic Therapy with Indocyanine Green Complements and Enhances Low-Dose Cisplatin Cytotoxicity in MCF-7 Breast Cancer Cells. *Mol. Cancer. Ther.* **2004**, *3*, 537–544.
57. Mamoon, A. M.; Gamal-Eldeen, A. M.; Ruppel, M. E.; Smith, R. J.; Tsang, T.; Miller, L. M. *In Vitro* Efficiency and Mechanistic Role of Indocyanine Green as Photodynamic Therapy Agent for Human Melanoma. *Photodiagn. Photodyn. Ther.* **2009**, *6*, 105–116.
58. Tseng, W. W.; Saxton, R. E.; Deganutti, A.; Liu, C. D. Infrared Laser Activation of Indocyanine Green Inhibits Growth in Human Pancreatic Cancer. *Pancreas* **2003**, *27*, e42-5.
59. Urbanska, K.; Romanowska-Dixon, B.; Matuszak, Z.; Oszajca, J.; Nowak-Sliwinsk, P.; Stochel, G. Indocyanine Green as a Prospective Sensitizer for Photodynamic Therapy of Melanomas. *Acta Biochim. Pol.* **2002**, *49*, 387–391.
60. Viale, A.; Pelicci, P. G. Awaking Stem Cells from Dormancy: Growing Old and Fighting Cancer. *EMBO Mol. Med.* **2009**, *1*, 88–91.
61. Viale, A.; De Franco, F.; Orleth, A.; Cambiaghi, V.; Giuliani, V.; Bossi, D.; Ronchini, C.; Ronzoni, S.; Muradore, I.; Monestiroli, S.; *et al.* Cell-Cycle Restriction Limits DNA Damage and Maintains Self-Renewal of Leukaemia Stem Cells. *Nature* **2009**, *457*, 51–56.
62. Fossati, V.; Kumar, R.; Snoeck, H. W. Progenitor Cell Origin Plays a Role in Fate Choices of Mature B Cells. *J. Immunol.* **2010**, *184*, 1251–1260.
63. Pelayo, R.; Welner, R.; Perry, S. S.; Huang, J.; Baba, Y.; Yokota, T.; Kincade, P. W. Lymphoid Progenitors and Primary Routes to Becoming Cells of the Immune System. *Curr. Opin. Immunol.* **2005**, *17*, 100–107.
64. Greenberger, J. S.; Sakakeeny, M. A.; Humphries, R. K.; Eaves, C. J.; Eckner, R. J. Demonstration of Permanent Factor-Dependent Multipotential (Erythroid/Neutrophil/Basophil) Hematopoietic Progenitor Cell Lines. *Proc. Natl. Acad. Sci. U.S.A.* **1983**, *80*, 2931–2935.
65. Daley, G. Q.; Van Etten, R. A.; Baltimore, D. Induction of Chronic Myelogenous Leukemia in Mice by the P210bcr/abl Gene of the Philadelphia Chromosome. *Science* **1990**, *247*, 824–830.
66. Flors, C.; Fryer, M. J.; Waring, J.; Reeder, B.; Bechtold, U.; Mullineaux, P. M.; Nonell, S.; Wilson, M. T.; Baker, N. R. Imaging the Production of Singlet Oxygen *In Vivo* Using a New Fluorescent Sensor, Singlet Oxygen Sensor Green. *J. Exp. Bot.* **2006**, *57*, 1725–1734.
67. Barth, B. M.; Stewart-Smeets, S.; Kuhn, T. B. Proinflammatory Cytokines Provoke Oxidative Damage to Actin in Neuronal Cells Mediated by Rac1 and NADPH Oxidase. *Mol. Cell. Neurosci.* **2009**, *41*, 274–285.